JGR Atmospheres

RESEARCH ARTICLE
10.1029/2019JD031470

Special Section:
Community Earth System Model version 2 (CESM2) Special Collection

Impact of Cloud Physics on the Greenland Ice Sheet Near-Surface Climate: A Study With the Community Atmosphere Model

Jan T. M. Lenaerts[1], Andrew Gettelman[2], Kristof Van Tricht[3], Leo van Kampenhout[4], and Nathaniel B. Miller[5]

[1]Department of Atmospheric and Oceanic Sciences, University of Colorado Boulder, Boulder, CO, USA, [2]National Center for Atmospheric Research, Boulder, CO, USA, [3]Remote Sensing Unit, Flemish Institute for Technological Research (VITO),Mol, Belgium, [4]Institute for Marine and Atmospheric Research Utrecht, Utrecht University,Utrecht,The Netherlands, [5]CIRES, University of Colorado Boulder, Boulder, CO, USA

Abstract The Greenland Ice Sheet (GrIS) is losing mass in an accelerated fashion, which is for ˜60% dominated by an increase in surface melting. Clouds exhibit an important control on the GrIS surface energy balance and surface melt. Therefore, to better simulate present and future GrIS climate, it is essential to represent clouds correctly in climate models. Here we use ground (at Summit Station) and satellite remote sensing (from CloudSat-CALIPSO) observations to evaluate GrIS cloud characteristics in several versions of the Community Atmosphere Model (CAM) over the period 2007–2012. Cloud cover, phase, water path, and radiative effects over the GrIS vary widely across the atmosphere models. Thanks to the inclusion of new cloud physical parameterizations, that is, ice nucleation and prognostic precipitation, in the most recent CAM version (CAM6), this model, amongst the various CAM versions, is best able to represent GrIS clouds, summer temperatures, and surface melting. However, CAM6 shows excessive rainfall over the ice sheet, which is an important outstanding model bias. Our study demonstrates the importance of simulating realistic cloud properties to improve climate model simulations of GrIS climate and climate change.

Key Points:
- Clouds over the Greenland Ice Sheet are sensitive to cloud physical parameterizations
- Addition of ice nucleation and prognostic precipitation leads an overall good performance in the Community Atmosphere Model 6 (CAM6)
- CAM6 produces excessive liquid precipitation over Greenland

Correspondence to:
J. T. M. Lenaerts,
Jan.Lenaerts@colorado.edu

Citation:
Lenaerts, J. T. M., Gettelman, A., Van Tricht, K., van Kampenhout, L., & Miller, N. B. (2020). Impact of cloud physics on the Greenland Ice Sheet near-surface climate: a study with the Community Atmosphere Model. *Journal Geophysical Research: Atmospheres*, *125*, e2019JD031470. https://doi.org/10.1029/2019JD031470

Received 5 AUG 2019
Accepted 22 MAR 2020
Accepted article online 20 MAR 2020

The copyright line for this article was changed on 16 APR 2020 after original online publication.

1. Introduction

Clouds control the Earth's hydrological cycle by delivering precipitation to the surface. In addition, clouds regulate the Earth's climate by reflecting solar (shortwave) radiation from the top of the atmosphere and absorbing and re-emitting thermal (longwave) radiation from/to the surface (Ramanathan et al., 1989). In the polar regions, and averaged over the year, the longwave warming effect of clouds clearly dominates the shortwave cooling effect because of the high surface albedos and long winter season. However, the cloud radiational effect varies substantially spatially and across seasons; for example, the cloud shortwave cooling effect dominates during the melt season, acting to reduce surface melting overall (Hofer et al., 2017; Niwano et al., 2019; Ruan et al., 2019; Wang et al., 2018, 2019). Cloud cover frequency, structure, and phase all are important for determining the extent of cloud warming (Shupe et al., 2004); while, in general, cold and high clouds preferentially dim shortwave radiation, low-level and liquid-containing also tend to absorb longwave radiation. Particular cloud conditions are believed to contribute to recent extreme climate events in the Arctic. For example, anomalously low cloud coverage, particularly higher (>1 km above the surface) in the atmosphere, is believed to have invoked the extreme 2007 Arctic sea ice loss (Kay et al., 2008), while a near-surface liquid cloud layer has probably led to the unique surface melt event at Summit, Greenland (3,250 m above sea level) in July 2012 (Bennartz et al., 2013).

In response to amplified climate warming in the Arctic, the Greenland Ice Sheet (GrIS) as a whole has experienced a strong increase of surface melt since the early 1990s, and more than 60% of current GrIS mass loss is ascribed to an increase in surface runoff from melt (Van den Broeke et al., 2016). Since one third of the annual Greenland surface runoff can be directly attributed to clouds (Van Tricht et al., 2016), reliable climate model simulations of clouds, their effect on the GrIS surface radiation and precipitation, and their future changes are of crucial importance to estimate future GrIS climate and mass balance (Hofer et al., 2019; Lenaerts et al., 2019; Niwano et al., 2019).

Despite their importance for the Arctic climate, Polar cloud properties are poorly represented by state-of-the-art climate models. For instance, there is an order-of-magnitude spread of cloud liquid (LWP) and ice water path (IWP) in the Community Model Intercomparison Project 5 (CMIP5) model ensemble over Greenland (Lenaerts et al., 2017; Van Tricht et al., 2016). These model deficiencies are, apart from the crude resolution of these models in the horizontal (hundreds of kilometers) and vertical (hundreds of meters) dimensions, explained by biases in the representation of Polar cloud microphysical properties (Hofer et al., 2019).

One of these deficient CMIP5 models is the Community Earth System Model version 1 with the Community Atmosphere Model CAM5 (CESM1-CAM5, Hurrell et al., 2013). CAM5 has been shown to produce very little (supercooled) cloud liquid water over the polar regions (Lenaerts et al., 2017), including the GrIS (McIlhattan et al., 2017). This leads to underestimated surface downwelling longwave radiation (Miller et al., 2018), surface temperature (Kay et al., 2016), and GrIS surface melting, all of which are essential to understand polar surface climate and its recent changes. The recently released successor model and participatory model in CMIP6, CESM2, includes a new atmosphere model (CAM6) with improved cloud microphysical parameterizations, partly targeting an improved representation of polar clouds. In this study, we aim to isolate and focus on the atmospheric inputs onto the GrIS, in particular clouds, and use atmosphere/land-only simulations. All other aspects of GrIS climate and SMB in the fully coupled CESM2 model, including a detailed evaluation, are discussed in Van Kampenhout et al. (2020).

Evaluation and development of CAM5 and CAM6 (and other global atmospheric and Earth System Models) cloud microphysical schemes over the GrIS and the Arctic as a whole have so far been hampered by the lack of observational data. However, with the recent availability of cloud remote sensing data from CloudSat and Cloud-Aerosol Lidar and Infrared Pathfinder Satellite Observation (CALIPSO), satellites that are sensitive to cloud phase and give information on cloud radiative impacts, we can now thoroughly assess the performance of climate models in representing GrIS clouds.

Here we evaluate cloud properties and their impact on climate over Greenland of five versions of the Community Atmosphere Model (CAM), ranging from CAM4 to CAM6 and in-between versions that have differing cloud microphysical parameterizations. Comparisons are performed with the CloudSat-CALIPSO dataset as well as with detailed in situ surface-based observations at Summit Station in interior Greenland. This paper is outlined as follows: Section 2 describes the data and the model setup, Section 3 presents the results, and final Section 4 gives conclusions.

2. Model Simulations

2.1. Numerical Setup

Here we use the atmosphere-land version of the Community Earth System Model (CESM), which simulates the climate on a global scale at a resolution of 0.9 (latitudinal) x 1.25 (longitudinal) degrees. We use an Atmospheric Model Intercomparison Project (AMIP, Gates et al., 1999) style configuration, in which the ocean and sea-ice conditions, and greenhouse gas, volcanic, and aerosol forcings are prescribed from observations. The simulations are performed for the period 2007–2013 to overlap with the available measurements (see Section 3). Since this is a relatively short period, this does not allow us to analyze the long-term climate over Greenland in these simulations. Instead, we are solely interested in the sensitivity of the atmospheric and surface conditions over Greenland to the choice of cloud parameterizations. The fixed ocean and sea-ice conditions allow us to directly isolate the response of the atmosphere signal on such changes. In this version of CESM, the atmospheric model CAM (see below) is coupled to the Community Land Model version 5.

2.2. The Community Atmosphere Model

This study uses several versions of the CAM, all of which are the base CAM versions that were not tuned specifically for Greenland. An overview of the simulations is given in Table 1. CAM4 (Gent et al., 2011) features a simplified bulk cloud microphysics scheme (Rasch & Kristjánsson, 1998). CAM5 (Neale et al., 2010) significantly replaces the stratiform cloud microphysics with a two moment scheme (MG1, (Morrison & Gettelman, 2008), which also includes ice supersaturation (Gettelman et al., 2010) and a more advanced cloud macrophysics (fraction) scheme (Park et al., 2014). CAM5 also includes a prognostic aerosol model (Liu et al., 2012) and new formulations for radiation (RRTMG, (Iacono et al., 2000) and the boundary layer (Bretherton & Park, 2009). CAM4 and CAM5 are available as part of CCSM4 (Gent et al., 2011) and CESM1 (Hurrell et al., 2013), respectively, and both models have been used in the CMIP5.

Table 1
Overview of the CAM Simulations and Their Cloud-Relevant Parameterizations Used in This Study

Name	Aerosols	Microphysics	PBL	Radiation	Mixed-Phase Ice Nucleation
CAM4	Bulk	R98	H93	C01	No
CAM5	3 modes	MG1	UW	RRTMG	No
CAM6	4 modes	MG2	CLUBB	RRTMG	Yes
CAM6-ice	4 modes	MG2	CLUBB	RRTMG	No
CAM6-clubb	4 modes	MG2	UW	RRTMG	Yes
CAM6-mg2	4 modes	MG1	CLUBB	RRTMG	Yes

Note. R98 refers to Rasch and Kristjánsson (1998), H93 to Holtslag and Boville (1993), and C01 to Collins (2001). Refer to the text for additional details.

The latest version of CAM, CAM6 (Gettelman et al., 2019), has a changed formulation of several components of the atmosphere relative to CAM5. The description of dust aerosol has been changed with respect to CAM5, with a new description of dust erodability and a change in fine mode fraction from 3.2% to 1.1% (Albani et al., 2015). The model has been changed from 30 levels (CAM5) to 32 levels (CAM6) to more closely match the stratospheric version of CAM. In addition, the modal aerosol model now includes a fourth mode for black carbon (MAM4, Liu et al., 2016). The aerosol mode widths are altered as described by Mills et al. (2016) to accommodate the evolution of stratospheric sulfur aerosol. In addition, three important changes for GrIS clouds have been incorporated, all of which are tested individually in this paper. To do so, we use three CAM6 sensitivity simulations besides the default CAM6 version, each of which with one component that separates CAM5 and CAM6 removed. In these three simulations, we test the sensitivity of the addition of three important components to CAM6 relative to CAM5, that is, (1) mixed-phase (we expect most of the liquid-containing clouds over Greenland to be mixed-phase, as opposed to containing only liquid water) ice nucleation developed by Hoose et al. (2010) and improved by Wang et al. (2014), denoted with "CAM6-ice" (i.e., CAM6 minus ice); (2) a unified moist turbulence scheme, which replaces the previous boundary layer, shallow convection, and cloud schemes, called Cloud Layers Unified By Bi-normals (CLUBB, Bogenschutz et al., 2013), denoted with "CAM6-clubb"; and (3) the second version of Morisson-Gettelman microphysics (MG2, Gettelman et al., 2015) including a prognostic representation of precipitation (snow and rain), referred to with "CAM6-mg2." Through consistently removing a single component from the CAM6 code base, we can robustly assess the affects of each of these individually on the simulation of clouds over Greenland.

3. Observational Data

In this study, we evaluate the model results with recent surface-based observational data from Summit, Greenland, and remote sensing data from CloudSat-CALIPSO. Both data sets are briefly described below.

3.1. Summit

Summit Station is located in central Greenland (72.6°N, 38.5°W) at approximately 3,250 m above sea level. The relatively homogeneous landscape surrounding Summit Station provides the opportunity to use ground-based measurements to represent a larger area in the accumulation zone. Hence, detailed measurements of cloud properties and surface radiation are compared to coarser spatial resolution satellite products and model simulations. For example, the surface height of the CAM grid point closest to the location of Summit is 3,132 m, close to the actual elevation of Summit station.

The Swiss Federal Institute of Technology Zürich records measurements of shortwave and longwave radiation at 2 m above the surface. Thermal emission (4.5-40 μm) originating from the atmosphere and the surface are measured by upward facing and downward facing pyrgeometers. A pair of pyranometers measure the upwelling and downwelling solar irradiance (200–3600 nm). A correction is applied to the downwelling longwave measured value as discussed in Miller et al. (2015). The uncertainty for longwave radiation measurements is $\sim$5 Wm^{-2} (Gröbner et al., 2014).

Ground-based measurements, collected as part of the Integrated Characterization of Energy, Clouds, Atmospheric State, and Precipitation at Summit (ICECAPS) project, capture the cloud presence and their microphysical properties (Shupe et al., 2013). Liquid water path (LWP) and precipitable water vapor (PWV)

is retrieved using four channels (23.8, 31.4, 90.0, and 150.0 GHz) from a pair of microwave radiometers, similar to Turner et al. (2007). The physical retrieval of LWP and PWV has uncertainties of ~3-5 gm^{-2} and 0.3 mm, respectively. Temperature and humidity profiles above Summit are used as input to the rapid radiative transfer model (Clough et al., 2005, RRTM) in order to estimate what the radiative flux at the surface would be if the overlying atmosphere was hydrometeor-free. Cloud radiative forcing is calculated for each broadband component by subtracting the modeled clear-sky flux from a corresponding measured all-sky flux. Cloud radiative forcing and LWP estimates are reported for the period January 2011–October 2013, as detailed in Miller et al. (2015). Finally, the ground-based values of broadband radiative fluxes, cloud radiative forcing, and LWP are averaged by month to create an annual cycle to be used for model evaluation purposes. Here we assume that the observations are representative for the 2011–2013 period and use the overlapping period in our simulations in the comparison.

3.2. Automatic Weather Stations

To provide additional observations of downwelling fluxes at the surface, we use measurements collected by Programme for Monitoring of the Greenland Ice Sheet (PROMICE) Automatic Weather Stations (AWSs) distributed across the GrIS (Van As et al., 2011). Radiation measurements on PROMICE stations are obtained by a Kipp & Zonen CNR1 or CNR4 radiometer. Monthly means are calculated from daily means if more than 24 daily means are available. From the original 25 PROMICE AWSs available, we retained data of the eight stations for which the elevation in CESM was within 200 m of the station elevation. For these stations and for each month, we averaged the downwelling fluxes across all available years (varying from one up to 11 years in the period 2008–2019) to yield a monthly "climatology" of downwelling fluxes.

3.3. Remote Sensing

CloudSat and Cloud-Aerosol Lidar and CALIPSO were launched in 2006 to join the A-Train, a sun-synchronous satellite constellation flying at an altitude of 705 km above the Earth (L'Ecuyer & Jiang, 2010). Until 2016, CloudSat and CALIPSO have been only 15 seconds apart in the constellation and observe the atmosphere below almost simultaneously.

CloudSat carries the 94-GHz Cloud Profiling Radar (CPR) that was designed to detect cloud signals and precipitation. The vertically resolved radar reflectivity factors are used to retrieve vertical profiles of liquid and ice water contents and precipitation rates at a vertical resolution of 240 m (Stephens et al., 2009). The drawback of the cloud penetrative capacities of the CPR is its limited sensitivity to smaller particles (Wang & Sassen, 2001), rendering it unsuitable for the detection of optically thin ice clouds or supercooled liquid cloud layers. The Cloud-Aerosol LIdar with Orthogonal Polarization (CALIOP) instrument aboard CALIPSO is with its shorter wavelengths of 532 and 1064 nm specifically designed to be sensitive to optically thin ice clouds and supercooled liquid droplets, abundant features in Polar atmospheres. Near-simultaneous observations from space by both radar (CPR) and lidar (CALIOP) therefore provide a near-complete view on cloud properties throughout the atmosphere at a near-global scale, including the polar regions.

In the level-2 "Combined Radar and Lidar Cloud Scenario Classification Product" product (2B-CLDCLASS-LIDAR), these lidar and radar observations are combined to give the best estimate of vertical cloud boundaries of up to 10 different layers, including cloud phase information for each layer (ice, liquid, or mixed-phase) (Wang & Sassen, 2001). All 2B-CLDCLASS-LIDAR data from 2007–2010 over Greenland were resampled to a 2° by 2° grid and multiyear averages of vertically resolved cloud fraction (ice, liquid, and total) were calculated for each gridbox at the original 240mCloudSat vertical resolution.

The level-2 *Fluxes and Heating Rates* algorithm (2B-FLXHR-LIDAR) combines these vertical profiles of cloud liquid and ice water contents with atmospheric temperature and humidity profiles from ECMWF ERA-Interim reanalyses to constrain a two-stream radiative transfer model (RTM, Henderson et al., 2013). Information on surface albedo and emissivity data is retrieved from the International Geosphere-Biosphere Programme (IGBP) global land surface classification. The RTM calculates broadband radiative fluxes at 126 vertical levels, the original resolution of the merged CloudSat/CALIPSO cloud observations. The radiative fluxes of the 2B-FLXHR-LIDAR algorithm have been extensively evaluated on both the global scale (Henderson et al., 2013) as well as more specifically in polar regions (Van Tricht et al., 2016). Here we use a modified version of the original R04 product with specific improvements in low-level liquid-containing clouds over polar regions (Van Tricht et al., 2016), which formed the basis for the new R05 product version (Matus & L'Ecuyer, 2017). Monthly mean downwelling surface radiative fluxes were calculated using 2007–2010 2B-FLXHR-LIDAR data resampled to a 2° by 2° grid.

Table 2
Annual Mean (2007-2013) Low, Middle, High, and Total Cloud Coverage (%) Over Greenland (Excluding North of 82°N, Where We Have no Observations) According to the CAM Simulations and CloudSat-CALIPSO Observations

	Low	Middle	High	Total
CAM4	25±3	30±2	15±2	43±2
CAM5	34±4	51±4	45±1	67±4
CAM6	41±4	67±4	55±1	81±3
CAM6-ice	42±5	64±4	50±3	78±4
CAM6-clubb	33±3	57±2	53±3	74±2
CAM6-mg2	33±5	58±5	48±4	72±5
Obs (Van Tricht et al., 2016)				67±5

Note. The stated uncertainty in the observations (which are only available for total cloud cover) is adopted from the statistical uncertainty associated with the CloudSat-CALIPSO 2B-CLDCLASS-LIDAR product (http://www.cloudsat.cira.colostate.edu/sites/default/files/news/CloudSat_Algorithm_Uncertainties_Synthesis.pdf).

3.4. RACMO2

To evaluate near-surface temperatures, precipitation, and surface melt in the CAM simulations, we use output of the Regional Atmospheric Climate MOdel 2 (RACMO2, Noël et al., 2018). Although RACMO2 is an atmospheric model itself, and potentially prone to cloud-related biases in near-surface and SMB parameters, we opt to use it in this study because (1) it provides a high-resolution (1 km), gridded, and continuous data set for the period 2007-2012 that overlaps with our CAM simulations of near-surface parameters over the entire GrIS and (2) RACMO2 has been evaluated in detail, and compares very well, with available in situ weather, radiation, and SMB observations on the GrIS (Ettema et al., 2010; Lenaerts et al., 2012; Noël et al., 2018; Van Angelen et al., 2012).

4. Results

4.1. Cloud Cover, Phase, and Structure

We start our analysis with the comparison of cloud cover frequency over Greenland in the different CAM simulations. For the model, we discriminate between low (CAM variable "CLDLOW," <3 km above sea level), mid-level (CAM variable "CLDMED," 3-7 km above sea level), and high-level (CAM variable "CLDHGH," >7 km above sea level) clouds because of the distinct radiative aspects of these clouds; for example, low-level clouds emit more longwave heat because they are warmer. Table 2 shows that the frequency of low-level cloud coverage increases from ~25% in CAM4 to ~34% in CAM5, and to ~42% in CAM6. The strong differences in low-level cloud coverage in the CAM6 sensitivity runs (~33-42%) indicates that low-level clouds are particularly sensitive to the choice of atmospheric parameterization. The frequency of mid-level and high cloud coverage increases substantially from CAM4 to the CAM5 versions, with an approximate doubling in occurrence of mid-level cloud cover (~30 to ~51%) and a tripling of high-level clouds (~15 to ~45%). As a result, overall cloudiness (CAM variable "CLDTOT," which is a weighted average of low-, mid-, and high-level clouds) is about 1.5 times higher in CAM5 compared to CAM4 and more realistic (both around 67%) in comparison with the CloudSat-CALIPSO observations (Table 2). In the CAM6 runs, the frequency of the mid- and high-level cloud coverage further increases relative to CAM5, and total cloud cover varies from ~72 to ~81%, which indicates that CAM6 somewhat overestimates total cloud cover on the GrIS.

Next, we use the CloudSat-CALIPSO satellite product to evaluate the model simulations for the vertically integrated mass of cloud liquid water and cloud ice, the liquid water (LWP), and ice water path (IWP). Figure 1 shows that the CAM simulations produce significantly different LWP values over Greenland. In CAM4, LWP is higher than 20 gm^{-2} over the entire ice sheet, whereas CAM5 does not produce any LWP at all over large portions of the GrIS, with the exception of a narrow band along the coast (<10 gm^{-2}). CAM6 produces much more LWP than CAM5 (5-50 gm^{-2}), which is reduced in the three sensitivity simulations, especially in CAM6-mg2 and CAM6-ice. In comparison to the observations, which show that LWP ranges from 10 to 100 gm^{-2} over the GrIS, the LWP is strongly overestimated in CAM4 and underestimated in CAM5. CAM6 and CAM6-clubb best reproduce observed LWP, indicating that the ice nucleation and MG2

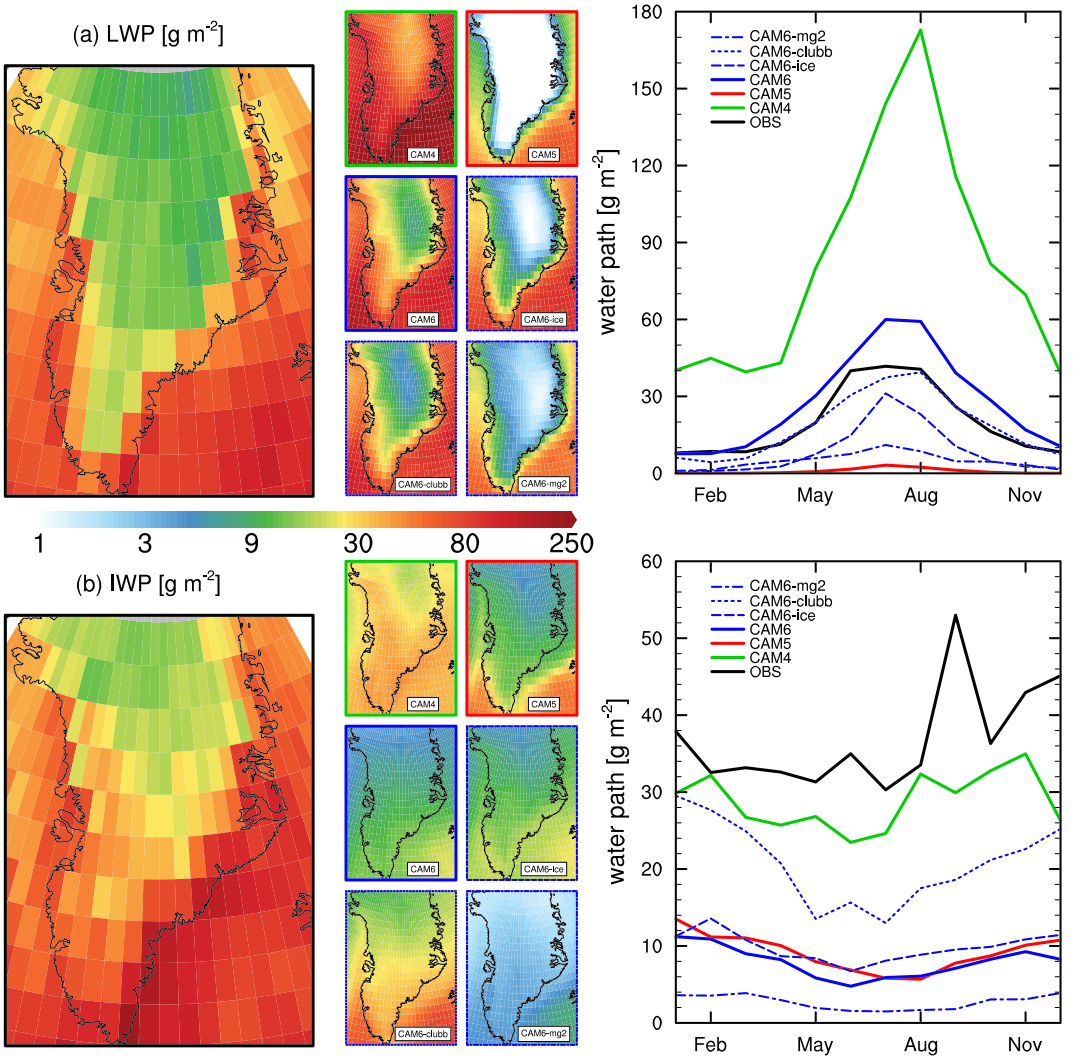

Figure 1. Annual mean (2007-2010) liquid (a) water and (b) ice water path according to the observations (large panels) and the CAM simulations (small panels). Note the exponential scale. The seasonal cycle of the mean LWP and IWP on Greenland is shown on the right.

changes are responsible for improved performance. The seasonal cycle of Greenland LWP shows a clear summer maximum, both in the observations (~10 gm^{-2} in winter to ~60 gm^{-2} in peak summer) and in the models. The CAM4 overestimation persists throughout the year (3–4 times higher than the observations), whereas CAM5 only shows a marginal amount of LWP in summer (<5 gm^{-2}). The performance of CAM6 is especially good in winter, whereas summer LWP appears slightly overestimated. The good representation of cloud LWP over Greenland in CAM6 can be explained by the combination of including of the MG2 cloud microphysical scheme and by allowing for mixed-phase ice nucleation: compared to CAM6, both CAM6-ice and CAM6-mg2 show lower LWP values over Greenland but simulate higher LWP than CAM5. In contrast, CAM6-clubb shows most realistic LWP values over the GrIS.

The observations at Summit Station (Figure 2a) confirm these findings. The observations indicate maximum LWP values over Summit of ~25 gm^{-2} in July, with values of 2-5 gm^{-2} in winter. CAM4 severely overestimates LWP in all seasons with a factor of five, whereas CAM5 simulates virtually zero LWP (<1 gm^{-2}) over Summit. CAM6 shows the best agreement with observations, with values of 2-5 gm^{-2} in winter, although summer LWP is slightly overestimated, which is consistent with the GrIS-wide results. Agreement with observations degrades in all CAM6 sensitivity simulations, especially in those without MG2 microphysics (CAM6-mg2), and without mixed-phase ice nucleation (CAM6-ice), in which LWP values remain below 10 gm^{-2} and 5 gm^{-2} in all seasons, respectively.

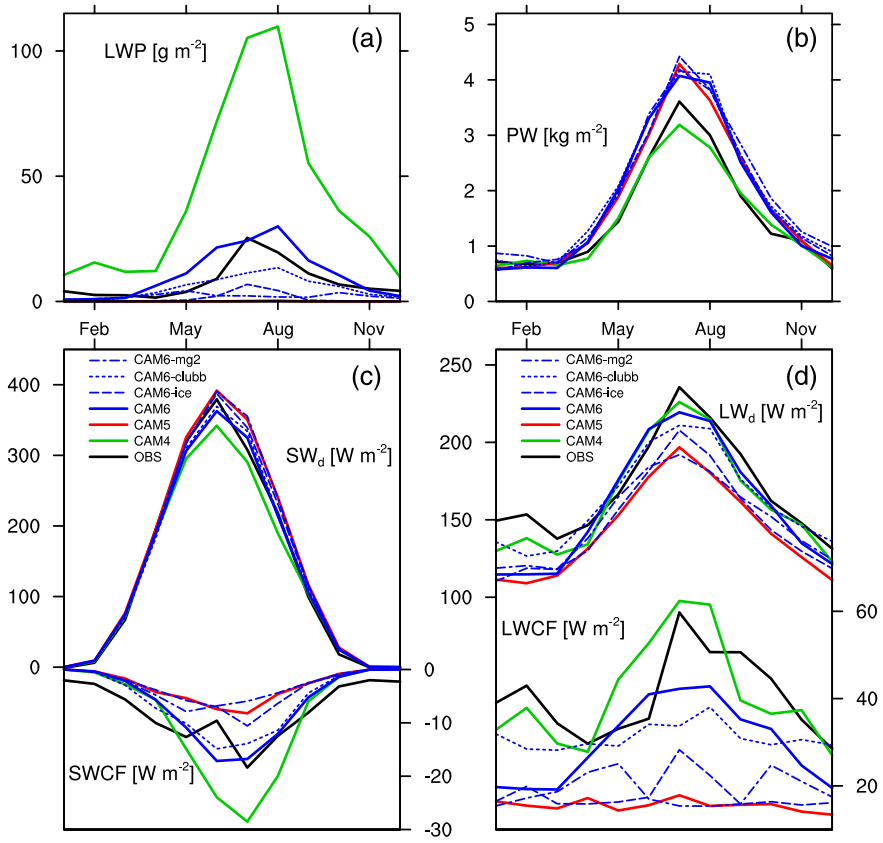

Figure 2. Seasonal cycle of different cloud-relevant parameters measured at Summit Station in 2011–2013, and simulated by the CAM runs. (a) Liquid water path (LWP); (b) precipitable water (PW); (c) downward shortwave radiation at the surface (SW_d) and shortwave cloud forcing (SWCF); (d) downward longwave radiation at the surface (LW_d) and longwave cloud forcing (LWCF).

IWP varies between ~10 gm^{-2} in the GrIS interior to >250 gm^{-2} in the southernmost coastal regions and shows a reverse seasonal cycle than LWP, with slightly higher values in winter (40-60 gm^{-2}) than in summer (~30 gm^{-2}). For IWP, we see similarities to LWP differences over the GrIS, with CAM4 showing much more IWP than CAM5 and all CAM6 versions (Figure 1). However, while it clearly overestimates GrIS LWP, CAM4 clearly outperforms all CAM5 and CAM6 simulations in its simulation of GrIS IWP. CAM5 and CAM6 underestimate IWP with a factor of 3 to 6. Interestingly, we see a different signal than for LWP, with the original CAM5 producing similar IWP amounts than the CAM6 simulation. The CAM6-clubb simulation produces the highest IWP values over the GrIS and approaches the observational estimates the best of all CAM5 and CAM6 simulations.

The CloudSat-CALIPSO data set allows not only for an evaluation of the vertically integrated cloud characteristics, but also permits to analyze the simulated vertical cloud structure. Here we demonstrate this by showing the vertical cloud structure along an east-west transect along the 72.5°N parallel (crossing the location of Summit station), as shown in Figure 3.

Liquid-containing (i.e., mixed-phase) clouds occur >10% over large portions of the GrIS, especially over the interior, at heights up to 5 km, and closer to the surface than ice-only clouds. Interestingly, we see a bipolar pattern on both sides of the ice sheets, with less liquid-containing clouds over the sloping edges of the ice sheet. We speculate that this is related to the surface wind conditions: on the ice sheet edges, strong katabatic winds are developed close to the surface (Gorter et al., 2014) while dry air is entrained from the higher boundary layer towards the surface, preventing the formation of liquid-containing clouds. As alluded to previously, CAM5 simulates no liquid clouds over Greenland, except over the coastal areas. In CAM6, some liquid clouds are present over the western part of the ice sheet, extending to the interior, and close to the surface. No liquid clouds are simulated over the eastern edge of the ice sheet.

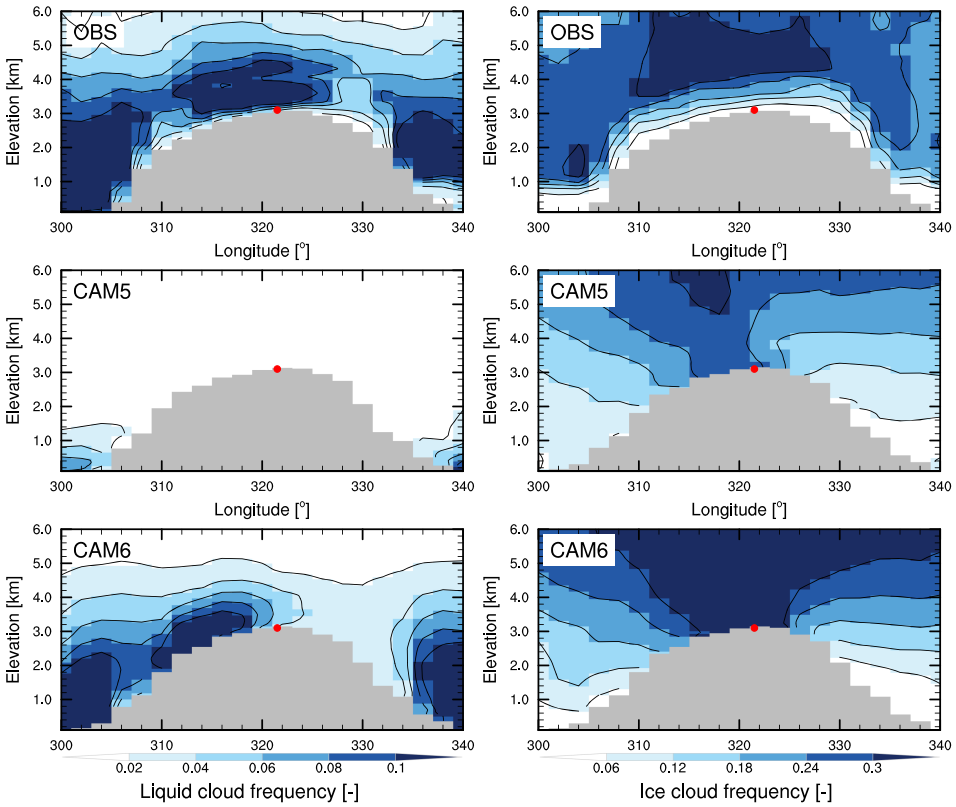

Figure 3. Cross section of the annual mean (2007–2012) frequency of liquid-containing clouds (left, unitless) and ice clouds (right, unitless) from west to east across Greenland at 72.5° north in the observations (CloudSat-CALIPSO), CAM5, and CAM6. The location of Summit Station is denoted with the red dot. CAM4 profiles are not available since they are not part of the model output, and the CAM6 sensitivity simulations are not shown since they show comparable or worse performance than CAM6 relative to the observations.

The observations show that ice clouds occur more than 30% of the time above the Greenland ice sheet, mostly at elevations between 1 and 3 km above the ice sheet surface. Closer to the surface, the frequency of ice clouds rapidly decreases. Ice clouds are found more regularly on the west side of the ice sheet than on the east side because the prevalent, mid-to-upper-tropospheric (500 mb and above) atmospheric flow originates from the west to southwest, which leads to orographic cloud formation on the windward side of the ice sheet, and commonly clearer conditions on the leeward side. Both CAM5 and CAM6 indicate higher ice cloud cover frequencies over the western GrIS but fail to simulate the observed patterns in great detail. In agreement with the observations, both models show a higher ice cloud cover frequency (20%–30%) over the interior ice sheet than along the periphery. However, both models suggest that these clouds exist all the way to the surface, while the observations show a clear decrease in cloud cover frequency going from 1 km above the surface downward. Part of this discrepancy is likely related to CloudSat's inability to detect clouds close to the surface (the so-called “blind zone” up to 1200 m above the surface, Maahn et al., 2014), and CALIPSO rapid attenuation for liquid water, implying that water path in CloudSat-CALIPSO is reduced close to the surface. Overall, this result, in combination with the IWP results discussed above, suggest that the models overestimate the frequency of ice clouds over the interior GrIS but underestimate the total amount of cloud ice.

4.2. Surface Radiative Fluxes

Next, we focus on the evaluation of the downwelling radiative fluxes over the GrIS in the CAM simulations. Despite the lower cloud coverage over Greenland (Table 2, also at Summit (not shown)), CAM4 strongly underestimates downwelling shortwave radiation at Summit Station (Figure 2c), ~50 Wm^{-2} too low), a well-known and Arctic-wide model bias (Collins et al., 2006; Kay et al., 2011), and presumably connected with too optically thick mixed-phase clouds (Figure 2a). This shortwave radiation deficit has been largely resolved in CAM5 (English et al., 2014). This leads to a smaller magnitude and less biased negative shortwave

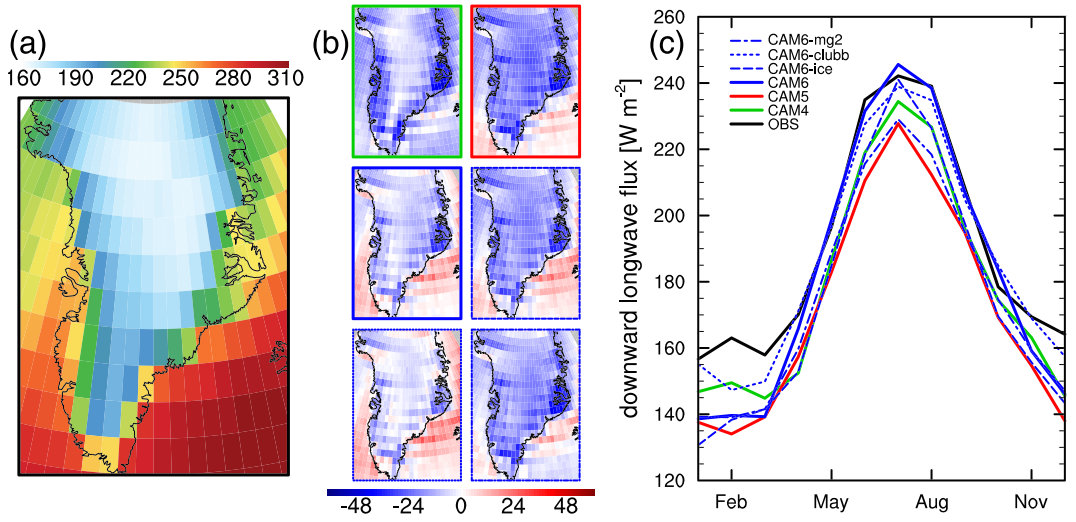

Figure 4. Annual mean (2007–2010) downward longwave radiation at the surface, according to the CloudSat-CALIPSO observations ("OBS," large panel), and the difference (model-observations) in the CAM simulations (small panels). The seasonal cycle of the mean Greenland downward longwave radiation is shown on the right.

cloud forcing (SWCF) in CAM5 (-5 Wm^{-2} in summer compared to ~-15 Wm^{-2} in the observations) than in CAM4, which strongly overestimates the magnitude of SWCF (<-30 Wm^{-2} in summer). In the CAM6 simulation, the SWCF is even more improved, yielding the best correspondence to the observations, especially in peak summer (SWCF around -18 Wm^{-2}). The default CAM6 model outperforms all CAM6 sensitivity simulations, which show a less negative SWCF in summer.

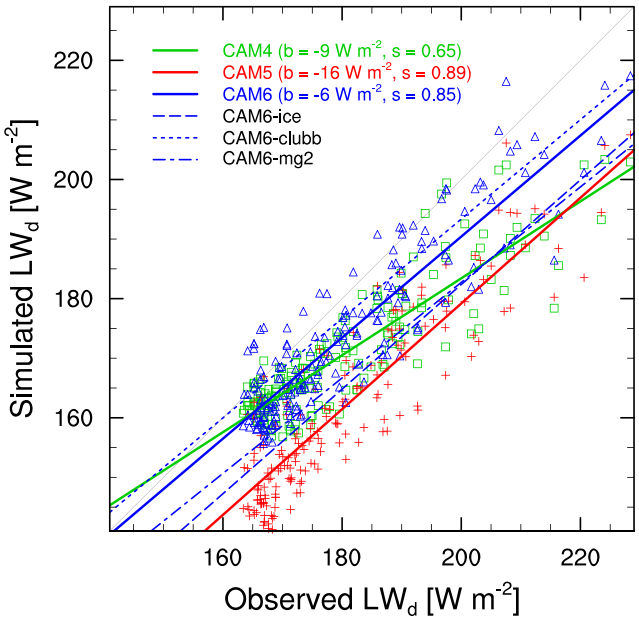

Figure 5. Modeled versus observed annual mean downward longwave radiation at the surface for each grid point on the GrIS according to CAM4 (green squares), CAM5 (red crosses), and CAM6 (blue triangles), and best linear fit between model and observations (colored lines, including the CAM6 sensitivity simulations). The statistics (b = mean bias; s = linear slope) are given in the legend for CAM4, CAM5, and CAM6. The thin black line shows the 1:1 correlation.

For longwave radiation, our results show that all models underestimate *LWd*, and that CAM4 simulates most realistic longwave radiation and cloud forcing (LWCF, Figure 2d), despite its excessive cloud liquid water (Figure 2d). In CAM5, *LWd* and LWCF are severely underestimated (up to 50 Wm^{-2} in summer) in lack of cloud water. This deficiency is greatly reduced in CAM6, in particular by the inclusion of mixed-phase ice nucleation and MG2 microphysics, as the CAM6-mg2 and CAM6-ice simulations show much reduced LWd and LWCF (similar to CAM5). We find the best correspondence with the observations in the default CAM6 simulation (10–20 Wm^{-2} underestimation). Including CLUBB only slightly reinforces the bias in longwave radiation and cloud forcing.

Because longwave downward radiation at the surface varies strongly over Greenland, depending on elevation and cloud conditions (Figure 4a), we use the satellite remote sensing data to evaluate the performance of the CAM versions over the entire sheet. All CAM simulations underestimate incoming longwave radiation at the surface, predominantly along the coasts (Figure 4b) and in winter (Figure 4c). In CAM4 and CAM6-clubb, winter LW_d show lowest biases (<10 Wm^{-2}) while CAM5 has a strong year-round negative bias (~ 13 Wm^{-2}). The good correspondence of CAM4 annual mean incident longwave radiation with observations (mean bias equaling -9 Wm^{-2}) originates from small biases over interior Greenland (where LW_d is low, Figure 5). However, CAM4 strongly underestimates LW_d in coastal areas, explaining the slope of the best linear fit of only 0.65 (Figure 5). CAM5 underestimates LW_d everywhere (mean bias -13 Wm^{-2}), leading to a higher slope of the best fit (0.89). The scatter in CAM6 is lowest (mean bias -6 Wm^{-2}), with very good model performance for LW_d values, and a minor underestimation of high LW_d values (in lower-elevation areas), leading to a slope of 0.85.

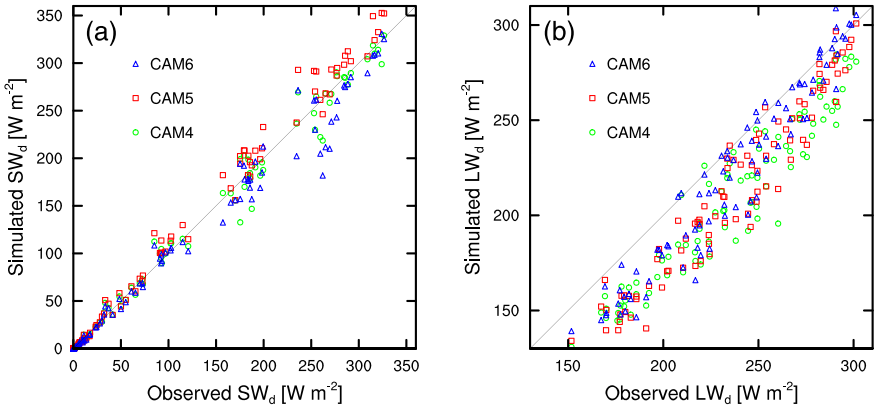

Figure 6. Scatter plots of monthly mean (averaged across all available measurement and simulation years) observed versus simulated (CAM4 in green, CAM5 in red, and CAM6 in blue) surface downwelling (a) shortwave and (b) longwave radiation. The thin diagonal black line shows the 1:1 line.

While CAM6-clubb sensitivity simulation shows equally good performance than CAM6, with a small overall bias (-3 Wm^{-2}), the CAM6-mg2 and CAM6-ice clearly perform worse, and biases in these versions are similar to those in CAM5. This result confirms once again that including ice nucleation and MG2 cloud physics have been essential to reduce GrIS LWd biases.

To supplement the comparison with satellite remote sensing, we compared the three main CAM simulations to measured downwelling fluxes by PROMICE stations. For shortwave radiation (Figure 6a), CAM4 and CAM6 underestimate shortwave radiation (with a mean bias of -2 and -6 Wm^{-2}, respectively), while CAM5 overestimates shortwave radiation (+8 Wm^{-2} bias), in accordance with our findings over Summit station (Figure 2c). With regard to longwave radiation, this analysis largely confirms the results of the comparison with the satellite remote sensing product. Both CAM4 and CAM5 show strong negative biases, especially at low LW_d values (Figure 6b), with mean biases of -27 and -25 Wm^{-2}, respectively, which are greatly reduced in CAM6 (mean bias -16 Wm^{-2}). The CAM6 sensitivity simulations (not shown) show similar behavior than reported in Figure 5.

The overall model performance in representing longwave cloud forcing at Summit Station and over the GrIS as a whole strongly resembles that of simulation of cloud liquid water (Figures 2a and 1), which indicates that the representation of cloud water path is essential to improve the SEB in climate models.

4.3. Impact on Surface Climate

The combined amount of shortwave and longwave radiation received by the GrIS surface varies significantly among the different CAM simulations. In winter, in absence of solar radiation, the surface energy balance (SEB) is primarily determined by longwave cooling. Clouds can act to reduce longwave cooling, especially if they contain liquid water. Associated with the wide discrepancy in cloud LWP amongst the CAM versions, we see differences in DJF temperatures of more than 5 K averaged across the GrIS (Figure 7), with the CAM4 temperatures (243 K on average) showing the closest resemblance to RACMO2 (245 K), and CAM5 showing a substantial cold bias (239 K), in part reduced in CAM6 (240 K). This is consistent with the best performance of CAM4 in representing GrIS and Summit station downwelling longwave radiation.

In summer, however, CAM4 near-surface temperatures (264 K) are clearly lower than those of RACMO2 (267 K) while CAM5 (266 K) and especially CAM6 (267 K) perform better than CAM4 (Figure 7). This discrepancy between winter and summer performance is likely related to the poor performance of CAM4 in representing downwelling shortwave radiation, illustrated by the excessively negative summer SWCF in CAM4 at Summit station (Figure 2c). In CAM5, compensating effects of too little (negative) SWCF and too little (positive) LWCF (Figure 2d) cause an overall reasonable net radiative energy and near-surface temperature. In contrast, CAM6 shows the best performance overall, with a combination of realistic SWCF and LWCF, although it still underestimates LWCF due to too little cloud LWP.

When the surface warms up to the melting point, the available energy is used to melt the snow, which illustrates that the onset and amount of melt is determined by the availability of radiative energy at the surface. Following the vast differences in the summer near-surface temperature and surface net radiation in

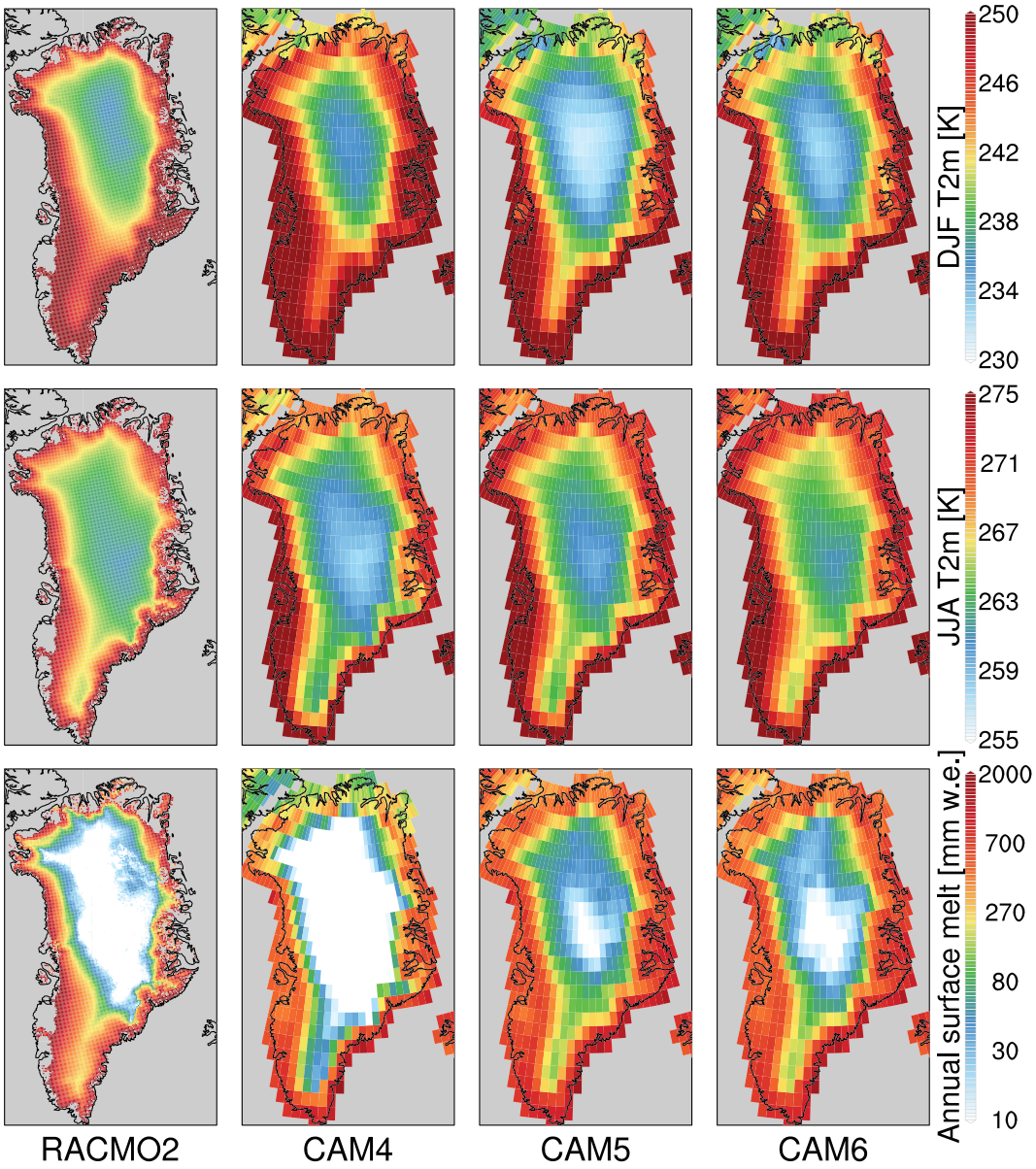

Figure 7. 2007–2012 mean winter (December-January-February, DJF; top row) and summer (June-July-August, JJA; middle row) near-surface temperature and annual surface melt (bottom row) according to RACMO2, CAM4, CAM5, and CAM6.

the various CAM simulations, the annual accumulated volume of surface melt varies substantially as well (Figure 7). While surface melt exceeds 1,000 kgm^{-2} (or millimeter water equivalent) per year along the edges of the GrIS in all simulations, the simulated differences in melt are high towards the interior. At elevations >2,000 m, the CAM6 simulation, with the most realistic summer temperatures, simulates surface melt over a large area of interior Greenland (5–50 kgm^{-2} per year), whereas CAM4 does not show any melt in most of the high areas in Greenland, in accordance with its cold bias in JJA temperatures. CAM5 surface melt looks similar to CAM6 despite the underestimation in LWCF and near-surface temperatures. This is likely related to the excessive shortwave radiation and cloud forcing in CAM5 (Figure 2) that supplies sufficient energy for melting during daytime. This result highlights that, especially in the interior of Greenland, the surface melt climate is strongly dependent on the representation of clouds and related radiation fluxes.

4.4. Impact on Precipitation

Along with causing differences in surface radiation, the choice of cloud physics in CAM also influences the amount and phase of precipitation on the GrIS. This is illustrated in Figure 8, which shows that there

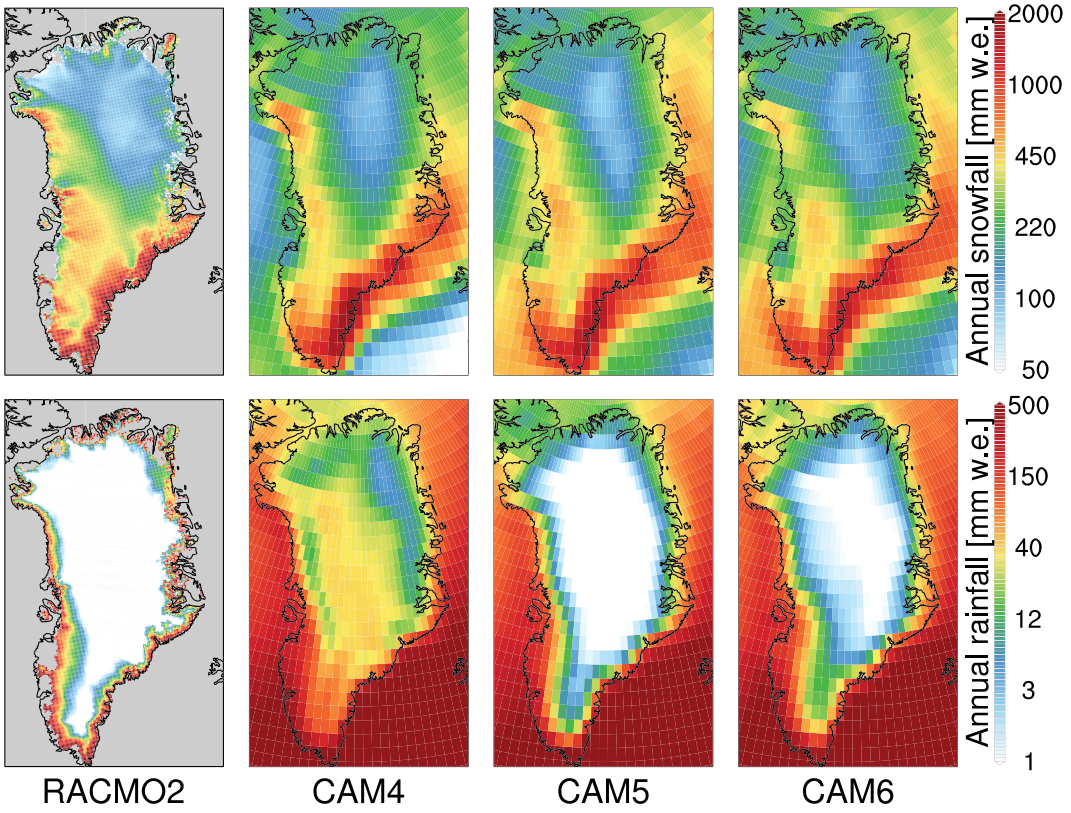

Figure 8. Annual solid (top) and liquid (bottom) precipitation in the CAM simulations in comparison with the regional climate model RACMO2 (Noel et al., 2015).

are relatively subtle differences between CAM versions in snowfall on the GrIS. The integrated snowfall amounts vary between 580 Gt/yr in CAM6, 642 Gt/yr in CAM5, and 661 Gt/yr in CAM4, that is, about 20% difference between CAM4 and CAM6. All the CAM versions represent the spatial patterns shown by RACMO2, which a band of high snowfall along the southeast GrIS coast (>1,000 mmw.e. per year) and very low snowfall amounts in the interior and northern GrIS (<100 mmw.e. per year). The differences in rainfall are very substantial, with CAM4 showing unrealistically high rainfall amounts across the GrIS, and CAM5 and CAM6 showing rainfall patterns that compare well to RACMO2, although they overestimate the spatial extent of the area where rainfall occurs (Figure 8).

5. Conclusions and Discussion

In this study, we evaluated the performance of six different recent versions of the Community Atmosphere Model (CAM) in simulating clouds over the Greenland ice sheet. The evaluation was performed by comparing the model output for a series of years in which high-quality station data (Summit Station, 2011–2013) and remote-sensing data (CloudSat-CALIPSO, 2007–2010) were available. CAM4 and CAM5, which were part of the most recent CMIP5 model ensemble of the IPCC AR5, both show large biases in Greenland clouds. CAM4 simulates relatively few clouds but excessive cloud liquid water, which leads to strong negative biases in the shortwave cloud forcing (i.e., too much (negative) shortwave cloud forcing). CAM5, on the other hand, generates no liquid water at all, resulting in largely deficient incoming longwave radiation at the surface due to insufficient positive longwave cloud forcing. The divergent cloud representation in the two models invokes a strong difference in incoming radiation over Greenland (20–30 Wm^{-2}), which evidently has consequences for the surface climate over Greenland. Vizcaíno et al. (2013) showed that the fully coupled climate model with CAM4 (CESM1) is able to realistically simulate present-day Greenland climate; however, an underestimation of incoming shortwave radiation (as in Figure 2a) was reportedly compensated by excessive longwave radiation, in line with the results presented here. In the same coupled model, but with CAM5 atmosphere, surface melt and associated runoff are strongly underestimated, which results in overestimated total surface mass balance (not shown).

CAM6, the most recent version of CAM, provides the best representation of cloud liquid water, longwave cloud forcing, summer near-surface temperature, and surface melting over the GrIS among the most recent CAM versions. In CAM5, which uses a previous version of MG (Morrison et al., 2005), cloud water is frozen rapidly, defined as an exponential function with decreasing temperature (Meyers et al., 1992; Gettelman et al., 2015). This explains the co-occurrence of high cloud ice values and very little cloud liquid water over the GrIS in CAM5.

Using sensitivity tests with various model improvements in CAM6 switched off, we have been able to isolate what updates in the cloud physics explain the reduced biases in CAM6 relative to CAM5. Our results show that the mixed-phase ice nucleation (which removes the Meyers 1992 scheme) and prognostic precipitation in MG2 both lead to a significantly reduced biases in cloud liquid and ice path over Greenland.

Mixed-phase ice nucleation describes immersion, contact, and deposition nucleation by a variety of aerosol types in mixed-phase clouds (Hoose et al., 2010). That implies that in relatively clean air, such as the above the GrIS, ice nucleation and cloud ice formation are limited. In CAM6, MG2 allows ice supersaturation, but since there is less cloud ice available from the reduced ice nucleation, there is less vapor deposition of liquid to ice in mixed-phase clouds, especially in the temperature range from -20 to 0°C. This explains the relative small IWP values and high LWP in CAM6 (Gettelman et al., 2019). In contrast, the addition of CLUBB does not improve the clouds over the GrIS in CAM6. Since CLUBB does not directly determine the cloud microphysical processes (but only the cloud macrophysics, or bulk condensate), CLUBB does not directly impact the relative distribution of cloud water and ice.

In addition, although their impact on surface radiation is very different, and they have different microphysical process sinks (Gettelman et al., 2019), cloud liquid and ice are physically linked. Most importantly, this physical link is established via ice nucleation and then the Wegener-Bergeron-Findeisen (WBF) process, which leads to cloud ice growth at the expense of supercooled liquid in mixed-phase clouds once ice has formed. Because ice will then grow faster, it will have a shorter lifetime. The WBF process is then a regulator of total water sink processes. This indicates that the biases of cloud LWP and IWP in the different CAM versions are related. Note that the WBF process is only represented in CAM5 and CAM6, while CAM4 has a fixed temperature ramp between liquid and ice. Thus, the realistic IWP but excessive LWP in CAM4 is likely associated with a phase distribution as a function of temperature in the Arctic that does not match observations. However, for CAM5, cloud LWP is virtually absent over Greenland but cloud IWP is less biased, indicative of a too efficient freezing (ice nucleation) and subsequent WBF process, as suggested by McIlhattan et al. (2017). Lastly, while CAM6 biases are lowest overall, the reasonable cloud LWP values in combination with generally too low IWP suggest that the ice nucleation and WBF process might be realistic in CAM6, but that the sink of cloud ice is too rapid due to excessive growth and/or excessive ice crystal sizes (leading to higher fall speed). All these processes are interlinked, which means further detailed cloud microphysical observations are necessary to disentangle the sources of the biases.

Overall, our results show that adaptations to the model cloud microphysics in CAM6 lead to significantly reduced cloud biases over Greenland due to better representation of the phase partitioning between liquid and ice. This indicates that advancing cloud microphysical parameterizations remains an essential step to improve representation of polar climate in climate models. However, substantial biases remain in CAM6, in particular the underestimation of cloud IWP with a factor of 3–4 over Greenland. In addition, we show that comprehensive observations of clouds and the radiative aspects on ice sheets, from the ground and from space, are essential in evaluating and improving climate models. To enable fully consistent comparisons between models and observations, future work should leverage satellite simulators in climate models (e.g., Bodas-Salcedo et al., 2011; Kay et al., 2018).

Our study focuses on cloud physics and does not consider other factors that potentially improve the simulation of GrIS near-surface climate and SMB in climate models. Among others, recent work has shown that enhancing horizontal resolution improves the representation of GrIS precipitation in CESM (Van Kampenhout et al., 2019) and also changes the distribution of (liquid-containing) clouds. In addition, correctly representing stable boundary layers and surface-based temperature inversions, which depends on model vertical resolution and stability corrections, is a challenge for many climate models (Holtslag et al., 2013), including CESM. For example, the negative bias in winter near-surface temperature in CAM6 is likely explained by the underestimated temperature inversion.

The findings presented here demonstrate that CAM6, which is the atmospheric component of the fully-coupled CESM2, improves the representation of cloud liquid and ice, as well as cloud radiative properties, in comparison to its predecessors CAM4 and CAM5. This is an important step towards providing realistic GrIS SMB in the fully coupled CESM2 model (including a dynamic ice sheet), which is documented in detail in Van Kampenhout et al. (2020).

Besides remaining cloud ice biases, an outstanding issue in CAM6 is the excessive amount of liquid precipitation over the ice sheet. We hypothesize that the higher mass of cloud liquid in CAM6 relative to CAM5 enhances the availability of rain. In addition, CAM6 lacks a freezing process of supercooled liquid at relatively warm temperatures ($\approx -10°C$ and higher). This hypothesis is confirmed by the simulation of supercooled drizzle over the polar regions in CAM6, a phenomenon that is not observed. Future model development work should focus on reducing the rainfall bias in CAM6 while, at the same time, retaining the relatively good performance in clouds and cloud radiative effects over the GrIS.

Acknowledgments
The CESM project is supported primarily by the National Science Foundation (NSF). This material is based upon work supported by the National Center for Atmospheric Research, which is a major facility sponsored by the NSF under Cooperative Agreement No. 1852977. Computing and data storage resources, including the Cheyenne supercomputer (https://doi.org/10.5065/D6RX99HX), were provided by the Computational and Information Systems Laboratory (CISL) at NCAR. Data are analyzed and graphics are designed using the NCAR Command Language (NCL, UCAR/NCAR/CISL/VETS, 2019). The model output of all simulations and variables discussed in this paper are available on Zenodo via http://doi.org/10.5281/zenodo.3687142. Data from the Programme for Monitoring of the Greenland Ice Sheet (PROMICE) and the Greenland Analogue Project (GAP) were provided by the Geological Survey of Denmark and Greenland (GEUS) at http://www.promice.dk.

References

Albani, S., Mahowald, N. M., Perry, A. T., Scanza, R. A., Zender, C. S., Heavens, N. G., et al. (2015). Improved dust representation in the Community Atmosphere Model. *Journal of Advances in Modeling Earth Systems*, *6*, 541–570. https://doi.org/10.1002/2013MS000279

Bennartz, R., Shupe, M. D., Turner, D. D., Walden, V. P., Steffen, K., Cox, C. J., et al. (2013). July 2012 Greenland melt extent enhanced by low-level liquid clouds. *Nature*, *496*(7443), 83–86. https://doi.org/10.1038/nature12002

Bodas-Salcedo, A., Webb, M. J., Bony, S., Chepfer, H., Dufresne, J.-L., Klein, S. A., et al. (2011). COSP: Satellite simulation software for model assessment. *Bulletin of the American Meteorological Society*, *92*(8), 1023–1043. https://doi.org/10.1175/2011BAMS2856.1

Bogenschutz, P. A., Gettelman, A., Morrison, H., Larson, V. E., Craig, C., & Schanen, D. P. (2013). Higher-order turbulence closure and its impact on climate simulations in the community atmosphere model. *Journal of Climate*, *26*(23), 9655–9676. https://doi.org/10.1175/JCLI-D-13-00075.1

Bretherton, C. S., & Park, S. (2009). A new moist turbulence parameterization in the Community Atmosphere Model. *Journal of Climate*, *22*(12), 3422–3448. https://doi.org/10.1175/2008JCLI2556.1

Clough, S. A., Shephard, M. W., Mlawer, E. J., Delamere, J. S., Iacono, M. J., Cady-Pereira, K., et al. (2005). Atmospheric radiative transfer modeling: A summary of the AER codes. *Journal of Quantitative Spectroscopy and Radiative Transfer*, *91*(2), 233–244. https://doi.org/10.1016/j.jqsrt.2004.05.058

Collins, W. D. (2001). Parameterization of generalized cloud overlap for radiative calculations in general circulation models. *Journal of the Atmospheric Sciences*, *58*(21), 3224–3242. https://doi.org/10.1175/1520-0469(2001)058<3224:POGCOF>2.0.CO;2

Collins, W. D., Bitz, C. M., Blackmon, M. L., Bonan, G. B., Bretherton, C. S., Carton, J. A., et al. (2006). The Community Climate System Model version 3 (CCSM3). *Journal of Climate*, *19*(11), 2122–2143. https://doi.org/10.1175/JCLI3761.1

English, J. M., Kay, J. E., Gettelman, A., Liu, X., Wang, Y., Zhang, Y., et al.(2014). Contributions of clouds, surface albedos, and mixed-phase ice nucleation schemes to arctic radiation biases in CAM5. *Journal of Climate*, *27*(13), 5174–5197. https://doi.org/10.1175/JCLI-D-13-00608.1

Ettema, J., van den Broeke, M. R., van Meijgaard, E., & van de Berg, W. J. (2010). Climate of the Greenland ice sheet using a high-resolution climate mode—l-Part 1: Evaluation. *The Cryosphere*, *4*(2), 511–527. https://doi.org/10.5194/tc-4-511-2010

Gates, W. L., Boyle, J. S., Covey, C., Dease, C. G., Doutriaux, C. M., Drach, R. S., et al. (1999). An overview of the results of the atmospheric model intercomparison project (AMIP I). *Bulletin of the American Meteorological Society*, *80*(1), 29–55. https://doi.org/10.1175/1520-0477(1999)080<0029:OOTRO>2.0.CO;2

Gent, P. R., Danabasoglu, G., Donner, L. J., Holland, M. M., Hunke, E. C., Jayne, S. R., et al. (2011). The Community Climate System Model version 4. *Journal of Climate*, *24*(19), 4973–4991. https://doi.org/10.1175/2011JCLI4083.1

Gettelman, A., Hannay, C., Bacmeister, J. T., Neale, R. B., Pendergrass, A. G., Danabasoglu, G., et al. (2019). High climate sensitivity in the community earth system model version 2 (CESM2). *Geophysical Research Letters*, *46*, 8329–8337. https://doi.org/10.1029/2019GL083978

Gettelman, A., Liu, X., Ghan, S. J., Morrison, H., Park, S., Conley, A. J., et al. (2010). Global simulations of ice nucleation and ice supersaturation with an improved cloud scheme in the Community Atmosphere Model. *Journal of Geophysical Research*, *115*, D18216. https://doi.org/10.1029/2009JD013797

Gettelman, A., Morrison, H., Santos, S., Bogenschutz, P., & Caldwell, P. M. (2015). Advanced two-moment bulk microphysics for global models. Part II: Global model solutions and aerosol-cloud interactions. *Journal of Climate*, *28*(3), 1288–1307. https://doi.org/10.1175/JCLI-D-14-00103.1

Gorter, W., van Angelen, J. H. H., Lenaerts, J. T. M., & van den Broeke, M. R. R. (2014). Present and future near-surface wind climate of Greenland from high resolution regional climate modelling. *Climate Dynamics*, *42*(5-6), 1595–1611. https://doi.org/10.1007/s00382-013-1861-2

Gröbner, J., Reda, I., Wacker, S., Nyeki, S., Behrens, K., & Gorman, J. (2014). A new absolute reference for atmospheric longwave irradiance measurements with traceability to SI units. *Journal of Geophysical Research: Atmospheres*, *119*, 7083–7090. https://doi.org/10.1002/2014JD021630

Henderson, D. S., L'Ecuyer, T., Stephens, G., Partain, P., & Sekiguchi, M. (2013). A multisensor perspective on the radiative impacts of clouds and aerosols. *Journal of Applied Meteorology and Climatology*, *52*(4), 853–871. http://doi.org/0.1175/JAMC-D-12-025.1

Hofer, S., Tedstone, A. J., Fettweis, X., & Bamber, J. L. (2017). Decreasing cloud cover drives the recent mass loss on the Greenland Ice Sheet. *Science Advances*, *3*, e1700584. https://doi.org/10.1126/sciadv.1700584

Hofer, S., Tedstone, A. J., Fettweis, X., & Bamber, J. L. (2019). Cloud microphysics and circulation anomalies control differences in future Greenland melt. *Nature Climate Change*, *9*(7), 523–528. https://doi.org/10.1038/s41558-019-0507-8

Holtslag, A. A. M., & Boville, B. A. (1993). Local versus nonlocal boundary-layer diffusion in a global climate model. *Journal of Climate*, *6*(10), 1825–1842. https://doi.org/10.1175/1520-0442(1993)006<1825:LVNBLD>2.0.CO;2

Holtslag, A. A. M., Svensson, G., Baas, P., Basu, S., Beare, B., Beljaars, A. C. M., et al. (2013). Stable atmospheric boundary layers and diurnal cycles: Challenges for weather and climate models. *Bulletin of the American Meteorological Society*, *94*(11), 1691–1706. https://doi.org/10.1175/BAMS-D-11-00187.1

Hoose, C., Kristjánsson, J. E., Chen, J.-P., & Hazra, A. (2010). A classical-theory-based parameterization of heterogeneous ice nucleation by mineral dust, soot, and biological particles in a global climate model. *Journal of the Atmospheric Sciences*, *67*(8), 2483–2503. https://doi.org/10.1175/2010JAS3425.1

Hurrell, J. W., Holland, M. M., Gent, P. R., Ghan, S., Kay, J. E., Kushner, P. J., et al. (2013). The community earth system model: A framework for collaborative research. *Bulletin of the American Meteorological Society*, *94*(9), 1339–1360. https://doi.org/10.1175/BAMS-D-12-00121.1

Iacono, M. J., Mlawer, E. J., Clough, S. A., & Morcrette, J.-J. (2000). Impact of an improved longwave radiation model, RRTM, on the energy budget and thermodynamic properties of the NCAR community climate model, CCM3. *Journal of Geophysical Research*, *105*(D11), 14,873–14,890. https://doi.org/10.1029/2000JD900091

Kay, J. E., L'Ecuyer, T., Gettelman, A., Stephens, G., & O'Dell, C. (2008). The contribution of cloud and radiation anomalies to the 2007 Arctic sea ice extent minimum. *Geophysical Research Letters*, *35*, L08503. https://doi.org/10.1029/2008GL033451

Kay, J. E., L'Ecuyer, T., Pendergrass, A., Chepfer, H., Guzman, R., & Yettella, V. (2018). Scale-aware and definition-aware evaluation of modeled near-surface precipitation frequency using CloudSat observations. *Journal of Geophysical Research: Atmospheres*, *123*, 4294–4309. https://doi.org/10.1002/2017JD028213

Kay, J. E., Raeder, K., Gettelman, A., & Anderson, J. (2011). The boundary layer response to recent Arctic sea ice loss and implications for high-latitude climate feedbacks. *Journal of Climate*, *24*(2), 428–447. https://doi.org/10.1175/2010JCLI3651.1

Kay, J. E., Wall, C., Yettella, V., Medeiros, B., Hannay, C., Caldwell, P., & Bitz, C. (2016). Global climate impacts of fixing the Southern Ocean shortwave radiation bias in the Community Earth System Model (CESM). *Journal of Climate*, *29*(12), 4617–4636. https://doi.org/10.1175/JCLI-D-15-0358.1

Lenaerts, J. T. M., Medley, B., van den Broeke, M. R., & Wouters, B. (2019). Observing and modeling ice sheet surface mass balance. *Reviews of Geophysics*, *57*, 376–420. https://doi.org/10.1029/2018RG000622

Lenaerts, J. T. M., van Den Broeke, M. R. R., van Angelen, J. H. H., van Meijgaard, E., & Déry, S. J. J. (2012). Drifting snow climate of the Greenland ice sheet: A study with a regional climate model. *The Cryosphere*, *6*(4), 891–899. https://doi.org/10.5194/tc-6-891-2012

Lenaerts, J. T. M., Van Tricht, K., Lhermitte, S., & L'Ecuyer, T. S. (2017). Polar clouds and radiation in satellite observations, reanalyses, and climate models. *Geophysical Research Letters*, *44*, 3355–3364. https://doi.org/10.1002/2016GL072242

Liu, X., Easter, R. C., Ghan, S. J., Zaveri, R., Rasch, P., Shi, X., et al. (2012). Toward a minimal representation of aerosols in climate models: Description and evaluation in the Community Atmosphere Model CAM5. *Geoscientific Model Development*, *5*(3), 709–739. https://doi.org/10.5194/gmd-5-709-2012

Liu, X., Ma, P. L., Wang, H., Tilmes, S., Singh, B., Easter, R. C., et al. (2016). Description and evaluation of a new four-mode version of the Modal Aerosol Module (MAM4) within version 5.3 of the Community Atmosphere Model. *Geoscientific Model Development*, *9*(2), 505–522. https://doi.org/10.5194/gmd-9-505-2016

L'Ecuyer, T. S., & Jiang, J. H. (2010). Touring the atmosphere aboard the A-Train. *Physics Today*, *63*(7), 36–41. https://doi.org/10.1063/1.3463626

Maahn, M., Burgard, C., Crewell, S., Gorodetskaya, I. V., Kneifel, S., Lhermitte, S., et al. (2014). How does the spaceborne radar blind zone affect derived surface snowfall statistics in polar regions? *Journal of Geophysical Research: Atmospheres*, *119*, 13,604–13,620. https://doi.org/10.1002/2014JD022079

Matus, A. V., & L'Ecuyer, T. S. (2017). The role of cloud phase in Earth's radiation budget. *Journal of Geophysical Research: Atmospheres*, *122*, 2559–2578. https://doi.org/10.1002/2016JD025951

McIlhattan, E. A., L'Ecuyer, T. S., & Miller, N. B. (2017). Observational evidence linking arctic supercooled liquid cloud biases in CESM to snowfall processes. *Journal of Climate*, *30*, 4477–4495. https://doi.org/10.1175/JCLI-D-16-0666.1

Meyers, M. P., Demott, P. J., & Cotton, W. R. (1992). New primary ice-nucleation parameterizations in an explicit cloud model. *Journal of Applied Meteorology*, *31*, 708–721. https://doi.org/10.1175/1520-0450(1992)031<0708:NPINPI>2.0.CO;2

Miller, N. B., Shupe, M. D., Cox, C. J., Walden, V. P., Turner, D. D., & Steffen, K. (2015). Cloud radiative forcing at Summit, Greenland. *Journal of Climate*, *28*(15), 6267–6280. https://doi.org/10.1175/JCLI-D-15-0076.1

Miller, N. B., Shupe, M. D., Lenaerts, J. T. M., Kay, J. E., de Boer, G., & Bennartz, R. (2018). Process-based model evaluation using surface energy budget observations in central Greenland. *Journal of Geophysical Research: Atmospheres*, *123*, 4777–4796. https://doi.org/10.1029/2017JD027377

Mills, M. J., Schmidt, A., Easter, R., Solomon, S., Kinnison, D. E., Ghan, S. J., et al. (2016). Global volcanic aerosol properties derived from emissions, 1990-2014, using CESM1(WACCM). *Journal of Geophysical Research: Atmospheres*, *121*, 2332–2348. https://doi.org/10.1002/2015JD024290

Morrison, H., Curry, J. A., & Khvorostyanov, V. I. (2005). A New double-moment microphysics parameterization for application in cloud and climate models. Part I: Description. *Journal of the Atmospheric Sciences*, *62*(6), 1665–1677. https://doi.org/10.1175/JAS3446.1

Morrison, H., & Gettelman, A. (2008). A new two-moment bulk stratiform cloud microphysics scheme in the community atmosphere model, version 3 (CAM3). Part I: Description and numerical tests. *Journal of Climate*, *21*(15), 3642–3659. https://doi.org/10.1175/2008JCLI2105.1

Neale, R. B., Chen, C.-C., Gettelman, A., Lauritzen, P. H., Park, S., Williamson, D. L., et al. (2010). Description of the NCAR community atmosphere model (CAM 5.0). NCAR Tech. Note NCAR/TN-486+ STR, 214.

Niwano, M., Hashimoto, A., & Aoki, T. (2019). Cloud-driven modulations of Greenland Ice Sheet surface melt. *Scientific Reports*, *9*(1), 10,380. https://doi.org/10.1038/s41598-019-46152-5

Noël, B., Van De Berg, W. J., Van Wessem, J. M., Van Meijgaard, E., Van As, D., Lenaerts, J. T. M., et al. (2018). Modelling the climate and surface mass balance of polar ice sheets using RACMO2—Part 1: Greenland (1958-2016). *Cryosphere*, *12*(3), 811–831. https://doi.org/10.5194/tc-12-811-2018

Park, S., Bretherton, C. S., & Rasch, P. J. (2014). Integrating cloud processes in the Community Atmosphere Model, version 5. *Journal of Climate*, *27*(18), 6821–6856. https://doi.org/10.1175/JCLI-D-14-00087.1

Ramanathan, V., Cess, R. D., Harrison, E. F., Minnis, P., Barkstrom, B. R., Ahmad, E., & Hartmann, D. (1989). Cloud-radiative forcing and climate: Results from the Earth Radiation Budget Experiment. *Science*, *243*(4887), 57–63. https://doi.org/10.1126/science.243.4887.57

Rasch, P. J., & Kristjánsson, J. E. (1998). A comparison of the CCM3 model climate using diagnosed and predicted condensate parameterizations. *Journal of Climate*, *11*(7), 1587–1614. https://doi.org/10.1175/1520-0442(1998)011<1587:ACOTCM>2.0.CO;2

Ruan, R., Chen, X., Zhao, J., Perrie, W., Mottram, R., Zhang, M., et al. (2019). Decelerated Greenland Ice Sheet driven by positive summer north atlantic oscillation. *Journal of Geophysical Research: Atmospheres*, *124*, 7633–7646. https://doi.org/10.1029/2019JD030689

Shupe, M. D., Intrieri, J. M., Shupe, M. D., & Intrieri, J. M. (2004). Cloud radiative forcing at the Arctic surface: The influence of cloud properties, surface albedo, and solar zenith angle. *Journal of Climate*, *17*(3), 616–628. https://doi.org/10.1175/1520-0442(2004)017<0616:CRFOTA>2.0.CO;2

Shupe, M. D., Turner, D. D., Walden, V. P., Bennartz, R., Cadeddu, M. P., Castellani, B. B., et al. (2013). High and dry: New observations of tropospheric and cloud properties above the Greenland Ice Sheet. *Bulletin of the American Meteorological Society*, *94*(2), 169–186. https://doi.org/10.1175/BAMS-D-11-00249.1

Stephens, G. L., Vane, D. G., Tanelli, S., Im, E., Durden, S., Rokey, M., et al. (2009). CloudSat mission: Performance and early science after the first year of operation. *Journal of Geophysical Research*, *114*, D00A26. https://doi.org/10.1029/2007JD009755

Turner, D. D., Clough, S. A., Liljegren, J. C., Clothiaux, E. E., Cady-Pereira, K. E., & Gaustad, K. L. (2007). Retrieving liquid water path and precipitable water vapor from the atmospheric radiation measurement (ARM) microwave radiometers. *IEEE Transactions on Geoscience and Remote Sensing*, *45*(11), 3680–3689. https://doi.org/10.5194/tc-6-1175-2012

UCAR/NCAR/CISL/VETS (2019). The NCAR Command Language (Version 6.6.2 [Software]. https://doi.org/10.5065/D6WD3XH5

Van Angelen, J. H., Lenaerts, J. T. M., Lhermitte, S., Fettweis, X., Kuipers Munneke, P., Van Den Broeke, M. R., et al. (2012). Sensitivity of Greenland Ice Sheet surface mass balance to surface albedo parameterization: A study with a regional climate model. *The Cryosphere*, *6*(5), 1175–1186. https://doi.org/10.5194/tc-6-1175-2012

Van As, D., Fausto, R. S., Ahlstom, A. P., Andersen, S. B., Morten, S. B., Citterio, M., et al. (2011). Programme for Monitoring of the Greenland Ice Sheet (PROMICE): First temperature and ablation records. *Geological Survey of Denmark and Greenland Bulletin*, *23*, 73–76.

Van Kampenhout, L., Lenaerts, J. T. M., Lipscomb, W. H., Lhermitte, S., Noël, B., Vizcaíno, M., et al. (2020). Present-day Greenland Ice Sheet climate and surface mass balance in CESM2. *Journal of Geophysical Research: Earth Surface*, *125*, e2019JF005318. https://doi.org/10.1029/2019JF005318

Van Kampenhout, L., Rhoades, A. M., Herrington, A. R., Zarzycki, C. M., Lenaerts, J. T. M., Sacks, W. J., & van den Broeke, M. R. (2019). Regional grid refinement in an Earth system model: Impacts on the simulated Greenland surface mass balance. *The Cryosphere*, *13*, 1547–1564. https://doi.org/10.5194/tc-13-1547-2019

Van Tricht, K., Lhermitte, S., Lenaerts, J. T. M., Gorodetskaya, I. V., L'Ecuyer, T. S., Noël, B., et al.(2016). Clouds enhance Greenland ice sheet meltwater runoff. *Nature Communications*, *7*, 10,266. https://doi.org/10.1038/ncomms10266

Van den Broeke, M. R., Enderlin, E. M., Howat, I. M., Kuipers Munneke, P., Noël, B. P. Y., van de Berg, W. J., et al. (2016). On the recent contribution of the greenland ice sheet to sea level change. *The Cryosphere*, *10*(5), 1933–1946. https://doi.org/10.5194/tc-10-1933-2016

Vizcaíno, M., Lipscomb, W. H., Sacks, W. J., van Angelen, J. H., Wouters, B., & van den Broeke, M. R. (2013). Greenland surface mass balance as simulated by the community earth system model. Part I: Model evaluation and 1850–2005 results. *Journal of Climate*, *26*(20), 7793–7812. https://doi.org/10.1175/JCLI-D-12-00615.1

Wang, Y., Liu, X., Hoose, C., & Wang, B. (2014). Different contact angle distributions for heterogeneous ice nucleation in the community atmospheric model version 5. *Atmospheric Chemistry and Physics*, *14*, 10411–10430. https://doi.org/10.5194/acp-14-10411-2014

Wang, Z., & Sassen, K. (2001). Cloud type and macrophysical property retrieval using multiple remote sensors. *Journal of Applied Meteorology*, *40*(10), 1665–1682. https://doi.org/10.1175/1520-0450(2001)040<1665:CTAMPR>2.0.CO;2

Wang, W., Zender, C. S., & van As, D. (2018). Temporal characteristics of cloud radiative effects on the Greenland Ice Sheet: Discoveries from multiyear automatic weather station measurements. *Journal of Geophysical Research: Atmospheres*, *123*, 311–348. https://doi.org/10.1029/2018JD028540

Wang, W., Zender, C. S., van As, D., & Miller, N. B. (2019). Spatial distribution of melt season cloud radiative effects over Greenland: Evaluating satellite observations, reanalyses, and model simulations against in situ measurements. *Journal of Geophysical Research: Atmospheres*, *124*, 57–71. https://doi.org/10.1029/2018JD028919